Published in final edited form as:
Biol Psychiatry. 2009 August 1; 66(3): 245–252. doi:10.1016/j.biopsych.2009.02.032.

DIFFUSE MICROSTRUCTURAL ABNORMALITIES OF NORMAL APPEARING WHITE MATTER IN LATE LIFE DEPRESSION: A DIFFUSION TENSOR IMAGING STUDY

Joshua S. Shimony[1], **Yvette I. Sheline**[2,1,3], **Gina D'Angelo**[4], **Adrian A. Epstein**[1], **Tammie L.S. Benzinger**[1], **Mark A. Mintun**[1,2], **Robert C. McKinstry**[1], and **Abraham Z. Snyder**[1,3]

[1] Mallinckrodt Institute of Radiology, Washington University School of Medicine, St. Louis, MO 63110

[2] Department of Psychiatry, Washington University School of Medicine, St. Louis, MO 63110

[3] Department of Neurology, Washington University School of Medicine, St. Louis, MO 63110

[4] Division of Biostatistics, Washington University School of Medicine, St. Louis, MO 63110

Abstract

Many recent studies have identified white matter abnormalities in late life depression (LLD). These abnormalities include an increased volume of discrete white matter lesions (hyperintensities on T2-weighted imaging) and changes in the diffusion tensor properties of water. However, no study of LLD to date has examined the integrity of white matter outside of discrete lesions, i.e., in normal appearing white matter. We performed T1- and T2-weighted imaging as well as diffusion tensor imaging (DTI) in depressed elderly subjects (n=73) and non-depressed control subjects (n=23) matched for age and cerebrovascular risk factors. The structural images were segmented into white matter, gray matter, cerebrospinal fluid and discrete white matter lesions. DTI parameters were calculated in white matter regions of interest after excluding the white matter lesions. Widespread LLD vs. control group differences were found, particularly in prefrontal regions, where the DTI abnormalities correlated with cognitive processing speed. These results suggest that further investigation is warranted to determine the basic pathophysiology and potential reversibility of LLD.

Keywords

Depression; MRI; Diffusion Tensor Imaging; Geriatrics; segmentation; LLD

INTRODUCTION

Several studies have identified white matter changes in late life depression (LLD). These changes include microstructural abnormalities determined by diffusion tensor imaging (DTI) and an increased volume of white matter hyperintensities (WMH) on T2-weighted imaging. However no study to date has separately examined these effects in the same population. Previous DTI studies of LLD have shown compromised structural integrity in white matter tracts linking limbic and dorsal frontal structures (1–3). We have recently found that the prevalence of WMH lesions is focally increased in these same tracts, which are known to mediate affective evaluation and executive control (4). This finding suggests that the strategic

Corresponding Author: Yvette Sheline, MD, Department of Psychiatry Box 8134, 660 S. Euclid Ave, St Louis MO 63110, Phone: 314-362-8422, Fax: 314-362-7599, yvette@npg.wustl.edu.

location of WMH may be critical to the pathophysiology of LLD. However, it remains unclear whether the predominant factor in the etiology of LLD is interruption of fiber tracts by lesions or more generally compromised white matter integrity.

Here, we used diffusion tensor imaging (DTI) in combination with segmentation of WMH to examine white matter integrity in late life depression. DTI measures the molecular motion (diffusion) of water in biological tissue (5). Mean diffusivity measures water diffusion averaged over all directions. Anisotropy refers to the degree to which diffusion is directionally dependent. Anisotropy characteristically is high in healthy white matter, as water tends to move parallel rather than perpendicular to fiber bundles. DTI abnormalities typically manifest as increased mean diffusivity (MD) and/or reduced anisotropy. DTI is capable of detecting subtle abnormalities in white matter that appears normal on standard T1- and T2-weighted imaging (6); hence the somewhat contradictory designation, “normal appearing white matter” (NAWM).

A novel feature of the present investigation was that discrete white matter hyperintensities (WMH) were segmented (4) and excluded from regional assessment of DTI measures, thereby confining the measurements to NAWM. We asked two questions of the DTI data: 1) Are white matter abnormalities detectable independent of WMH lesions? 2) If so, in which areas of the brain are they located? We compared a large group of LLD patients to a cohort of control subjects matched for age and cerebrovascular risk factors (7). We systematically sampled multiple brain regions to investigate the distribution of white matter damage. We hypothesized that evidence of structural damage would be found in multiple white matter regions that appear normal on T1- and T2-weighted imaging.

METHODS

Subjects

Depressed subjects (n=76) and non-depressed controls (n=23) aged 60 years and older with a wide range of cerebrovascular risk factors were recruited from an NIMH study “Treatment Outcome in Vascular Depression” to be part of the current NARSAD-sponsored project “Decreased White Matter Connectivity in Late Life Depression.” Patients and controls were recruited through advertising and physician referral to the Washington University Medical Center. Depressed and control subjects were matched for age (Mean = 68.6 ± 7.2, and Mean = 70 ± 5.9, respectively) and gender (71/29% female/male and 61/39% female/male, respectively). Patients and controls were evaluated by board-certified psychiatrists according to DSM-IV criteria for major depression in the former and a lifetime absence of psychiatric illness in the latter. All subjects were screened to rule out severe or unstable medical disorders (8), had Mini Mental Status Examination scores ≥ 24 (9), and had no history of other Axis I disorders prior to diagnosis of depression by SCID (Structured Clinical Interview for DSM4). All subjects provided written informed consent in accordance with the Washington University Institutional Review Board. All depressed patients were enrolled in a 12 week treatment course with sertraline. Prior to starting treatment patients completed all imaging and neuropsychological testing. All subjects were evaluated with the Montgomery-Asberg Depression Rating Scale (MADRS) (10) before and after therapy and were also evaluated using the Framingham Study cerebrovascular risk profile (CVR) (7). Depressed and control subjects were group-wise matched on age, gender, education and the Framingham CVR profile (see Table 1).

Subjects were also evaluated with a battery of neurophyschological tests. As previously described (8), these tests assessed several cognitive domains: language processing (Shipley Vocabulary test, the Boston Naming test, and the word reading condition of the Stroop task), cognitive processing speed (symbol-digit modality, color naming of the Stroop task, and Trails

A), working memory (digit span forward and backward, and ascending digits), episodic memory (word list learning, logical memory, constructional praxis, and the Benton visual retention test), and executive function (verbal fluency, Trails B, the color-word interference condition of the Stroop test, the initiation-preservation subscales of the Mattis Dementia Rating Scale, and categories completed from the Wisconsin Card sorting test).

Image Acquisition

All imaging was performed on a 1.5T Siemens Sonata scanner (Erlangen, Germany). Structural scans included a T1-weighted (T1W) sagittal, magnetization-prepared rapid gradient echo (MP-RAGE; repetition time (TR) = 1900 ms; inversion time (TI) = 1100 ms, echo time (TE) = 3.93 ms, flip angle = 15°, 1×1×1.25 mm voxels) and a T2-weighted (T2W) fast spin echo (TR = 4380 ms, TE = 94 ms, 1×1×3 mm). DTI was acquired using a locally modified echo planar imaging (EPI) sequence (TR = 7000 ms, TE = 113 ms, 2.0 mm isotropic voxels, 4.0 mm slice gap), conventional hexahedral (6 direction) encoding and three levels of diffusion sensitization (b-values = 400, 800, and 1200 s/mm^2). Contiguous coverage was obtained in three spatially interleaved acquisitions. Four complete DTI datasets were acquired in each participant. Total imaging time was approximately 90 minutes.

Image Registration

The first image-processing step was to define the spatial relationships between all images in terms of affine transforms computed by image registration. Multi-modality (e.g., T2W→T1W) image registration was accomplished using vector gradient measure (VGM) maximization (11). The first acquired, unsensitized (b = ~0 s/mm^2; I_0) DTI volume was registered to the T2W image; stretch and shear were enabled (12 parameter affine transform) to partially compensate for EPI distortion. Atlas transformation was computed *via* the T1W image, which itself was registered to an atlas representative target produced by mutual co-registration of MP-RAGE images from 12 normal, young adults. The atlas target conformed to the Talairach system (12) as implemented by Lancaster et al. (13). Algebraic composition of transforms (matrix multiplication) enabled resampling any data type in register with any other (14). Thus, ROI generated on anatomical images were resampled in register with the DTI data for purposes of DTI parameter measurement.

Head motion correction of the DTI data

Each DTI dataset included 19 volumes (18 diffusion sensitized + 1 unsensitized) assembled by collating slices from three interleaved scans. No attempt was made to correct for head motion between the interleaved slice scans. Each 19 volume dataset was motion corrected using a procedure that iteratively cycled through the following steps: (i) Align each volume to the geometric mean volume of each group of images sharing the same degree of sensitization (6 × b = 400 s/mm^2, 6 × b = 800 s/mm^2, 6 × b = 1200 s/mm^2, 1 × b = 0 s/mm^2). (ii) Recompute the geometric mean volume. (iii) Align each group geometric mean to the first acquired I_0 image. (iv) Algebraically compose transforms (volume→group geometric mean with group→I_0). Three cycles through the preceding steps yielded realignments with errors estimated by internal consistency to be less than 0.1 mm. All transforms were 9 parameter affine (rigid body + scanner axis stretch) computed by VGM maximization (11). The I_0 volumes of each DTI dataset were aligned using conventional intensity correlation maximization (15). The final, motion corrected result was obtained by algebraically composing all transforms (saved from the iterative procedure) and averaging all datasets after application of the composed transforms using cubic spline interpolation. The final resampling step output 19 volumes in spatial register with the I_0 volume of the first acquired DTI dataset.

Segmentation of individual anatomical images

The co-registered T1W and T2W structural images were segmented into regions representing cerebrospinal fluid, gray matter, white matter and WMH using a previously described semi-automated procedure (4) based on bi-spectral fuzzy class means (16). Artifactual intensity inhomogeneity was corrected prior to segmentation using a second order 3D polynomial model of the gain field (17). The gray matter/white matter (GM/WM) segmentation was used to individually define superficial white matter ROI sub-adjacent to standard cortical zones (see below). DTI measurements were performed in ROIs after exclusion of WMH voxels. The total WMH volume for each subject was used as an independent variable in statistical tests.

Definition of superficial white matter ROI

Superficial regions of interest (ROIs) were defined in the white matter sub-adjacent to major anatomical divisions of the cortex in both hemispheres of each participant. Cortical zones were selected on a standard surface atlas (18). The present selection of frontal regions is similar to that used by other investigators (19,20) and includes the superior frontal gyrus, middle frontal gyrus, inferior frontal gyrus, medial orbital frontal, lateral orbital frontal, dorsal cingulate, anterior cingulate, ventral cingulate, mesial fronto-polar cortex, and motor cortex. Additional regions were selected in the temporal lobe (medial temporal gyrus, fusiform gyrus, and auditory cortex), parietal lobe (somatosensory cortex and posterolateral intra parietal sulcus), and occipital lobe (occipital pole and the visual cortex). The zones depicted in Figure 2A were limited to the gyri to minimize ROI overlap in subsequent steps. For the purpose of the subsequent analysis the superficial pre-frontal regions were combined into a large pre-frontal region. Similarly, the superficial non-prefrontal regions were combined in a large non-prefrontal region.

The selected cortical zones (Figure 2A) were assigned a thickness of 3 mm to create standard 3D ROIs in atlas space. Then, for each subject, these standard ROIs were transformed to each individual's coordinate space and their intersection with the individually segmented cortical ribbon was computed. These individual results then were passed through the following automated steps (Figure 3): i) isotropic dilation by 2 mm ii) restriction of the dilated results to WM and iii) erosion by one voxel at GM boundaries to minimize partial volume effects in subsequent DTI measurements. ROI overlap was eliminated by assigning any shared voxels to the ROI with the nearest center of mass. Finally, each ROI was segmented into "normal appearing white matter" and WMH, and the WMH voxels were excluded. ROIs were visually inspected to confirm anatomic localization to normal appearing white matter at the conclusion of the automated processing.

Definition of deep WM ROI

Cubic 10 mm^3 ROIs were bilaterally placed in the deep WM of multiple cerebral lobes initially at standard atlas coordinates far removed from the cortical surface. These ROIs were in ventral, dorsal, and posterior frontal lobe, as well as temporal, and parietal lobe. Similar deep ROIs could not be placed in the occipital lobe because of its characteristically high degree of folding. The placement of each ROI was individually adjusted to ensure that only deep white matter was included. In addition, cubic ROIs (6 mm^3) were individually placed in the splenium and genu of the corpus callosum. The deep white matter ROIs in a representative subject are illustrated in Figure 2B.

DTI computations

The diffusion tensor and its 3 eigenvalues was calculated using log-linear regression in each voxel (5). Using standard methods the mean diffusivity was computed as the average of the 3 eigenvalues. Anisotropy was expressed as relative anisotropy (RA), which assumes values in

the range of 0 to 1 (21,22). Diffusion parameters were measured in individuals by averaging over voxels within each ROI, critically, excluding voxels previously identified as lesion (WMH). This procedure thus returned two DTI measures: relative anisotropy and mean diffusivity (RA and MD) evaluated in normal appearing white matter.

Statistical analysis of group differences and correlations

All statistical analyses were performed using Cytel Studio Version 8.0 for exact statistics and SAS Version 9.1 for the nonparametric statistics. Frequency matching by age and gender within the groups was chosen as the design. Thus, all statistical tests were adjusted by or stratified by age and gender, depending on the test. Age was categorized by terciles to ensure all statistical tests were consistent. Because of the unbalanced sample sizes (depressed vs. healthy control subjects in 3:1 ratio owing to recruitment strategy) the Wilcoxon-Mann-Whitney exact test was performed to determine if the mean of the regional DTI measures differed between the two groups stratified by age and gender. Partial Spearman correlation tests were performed to assess within-group relations between processing speed and regional DTI measures with adjustment for age and gender. The question of whether these associations were mediated by white matter lesion volume was investigated by computing correlations that were unadjusted vs. adjusted by this measure.

RESULTS

ROI diffusion parameter comparisons

Consistent depressed vs. control group differences were found in all pre-frontal regions (frontal ROIs excluding the motor ROI), in the other combined non-prefrontal regions (temporal, parietal, occipital, and motor ROIs), and in the deep white matter regions. Accordingly, in the interests of data reduction, DTI measures in anatomically related regions were combined. The consolidated results are presented in Table 2.

As is evident in Table 2, all combined regions showed statistically significant depressed vs. control group differences, with increased mean diffusivity (MD) in the depressed group. The prefrontal regions alone demonstrated significant relative anisotropy (RA) differences between depressed and controls, indicating a greater degree of microstructural abnormality in the prefrontal WM as compared to other WM in the brain.

DTI correlations with WMH volumes

In the depressed subjects significant Spearman rank-order correlation results were seen between most of the DTI parameters and WMH volume adjusted for age and gender (Table 3). These results were not seen in the control group, which demonstrated no significant correlations. This was true despite there being no significant difference between the groups in WMH volume, either over the whole brain or in any specific region.

DTI correlations with cognitive processing speed

In the depressed subjects, significant Spearman rank order correlations were seen between processing speed and prefrontal MD and RA adjusted for age and gender (Table 4A). Additional significant correlations were seen between processing speed and MD measured in the deep WM ROI and the CC. Similar correlations were not observed in the control group. WMH volume was significantly correlated with processing speed in the depressed ($r_S = -0.30$, $p = 0.0147$, $N = 67$) but not in the control group ($r_S = 0.28$, $p = 0.2288$, $N = 22$), suggesting that the relationship between cognitive impairment and DTI measures might be mediated (in a statistical sense) by WMH volume despite the fact that all DTI measures were obtained in NAWM. This question was examined by recalculating Table 4A with additional adjustment

for WMH volume (results listed in Table 4B). The only remaining significant Spearman correlation with processing speed was with MD in the prefrontal region.

Having found significant correlations between several variables (WMH volume, processing speed, and DTI measures in several ROIs) in the LLD group but not the control group, the question arose regarding whether these group differences were statistically reliable. We investigated this question using Bilker's CORANOVA (23), a bootstrap-based procedure suitable for evaluating the significance of non-parametric statistics, including Spearman rank order correlations. CORANOVA showed significant group differences in correlation between WMH volume and processing speed (p =.029). Similarly, the groups differed significantly in the correlation between deep WM MD and processing speed ($p < .005$).

DISCUSSION

The most notable design feature of the present study is segmentation of discrete white matter hyperintensities (WMH) and exclusion of these lesions from the DTI measurements. Since mean diffusivity is elevated and relative anisotropy is decreased within WM lesions, omitting the segmentation step (which currently is the norm in DTI studies) theoretically increases group differences in comparisons such as those reported in Table 5. However, retaining the lesions in WM ROIs means that observed DTI abnormalities could be attributable to the lesions. The present experimental design disambiguates interpretation of obtained results. Our finding of diffuse microstructural damage in normal appearing white matter suggests that WMH represent a "tip of the iceberg" phenomenon. In other words, the appearance of discrete lesions on conventional T1- and T2-weighted images implies that concomitant microstructural damage, currently detectable only by DTI, is present in NAWM. Thus we conclude that white matter abnormalities are detectable in NAWM outside of WMH.

Additional support for the view that WMH represent only a small portion of the overall white matter pathology comes from a neuropathological study of WMH imaged both pre- and post-mortem (24). Difference in the number of WMH lesions between depressed vs. control subjects was found exclusively in punctate (<3mm) rather than larger lesions. Data acquired in other laboratories indicate that the "tip of the iceberg" phenomenon is a characteristic of many conditions other than vascular depression, e.g., inflammatory demyelinating disease (25–29) and other neuropathologies (30–34).

We also addressed the question of location of brain white matter abnormalities. Our results are broadly consistent with previous findings of DTI abnormalities in LLD that emphasize prefrontal focality. Several previous DTI studies (summarized in Table 5) have reported white matter changes in late life depression compared to age-matched controls. In aggregate, these studies found lower white matter anisotropy in late life depression compared to age matched controls, primarily in the frontal lobes, with some studies also reporting significant changes in the temporal lobes, limbic areas and insula (1,2,35). One study found diffuse abnormalities throughout the brain (36). No prior study of LLD employed lesion segmentation and evaluation of diffusion properties in NAWM. Our results thus confirm prior findings of prefrontal white matter disease in LLD (Table 5), but we suggest that a more accurate description of the distribution of white matter disease in LLD would be that it is widespread (Table 2), although with a prefrontal emphasis. Unlike some other studies, we did not observe a consistent relation between severity of depression and white matter anisotropy (2). Nevertheless, a relation between the categorical diagnosis of depression and white matter disease is apparent in the robust effects listed in Table 2.

In addition, we found increased mean diffusivity (MD) in several ROIs including highly significant LLD vs. control group differences in prefrontal white matter. Only one previous

study (19) examined mean diffusivity but did not find LLD vs. control differences in any ROI. This discrepancy may be attributable to technical factors including longer imaging time and more elaborate preprocessing (e.g., head movement correction), which enhanced the sensitivity of the present methodology in comparison to prior studies. Increased mean diffusivity generally indicates elevated water content (6). In view of the established associations between cerebrovascular risk factors, white matter disease and depression ("vascular depression") (37–42), mean diffusivity increases in late life depression may represent loss of cellular membranes and intracellular compartments consequent to chronic ischemia.

It is noteworthy that in our previous study of WMH in LLD (4), no group differences were found in total WMH volume but the density of WMH was focally increased in specific white matter regions, including the superior longitudinal fasciculus, inferior longitudinal fasciculus, uncinate fasciculus and extreme capsule. This suggested that the emotional and cognitive deficits in LLD might arise because of interruption of certain key white matter pathways. Speculatively, the presently observed mean diffusivity changes in deep white matter could reflect disconnection and secondary Wallerian degeneration.

However, the present results also support the notion that there may be a distinct white matter pathopysiology that is diffusely present in normal appearing white matter and contributes to LLD irrespective of WMH. In support of this interpretation, CORANOVA showed significant group differences in the correlation between WMH volume and processing speed (p =.029). In other words, for a given WMH lesion in a depressed person there was a stronger influence on processing speed than in a matched control—even if that control had the same whole brain WMH burden. In addition, deep white matter mean diffusivity and WMH volume were highly correlated in depressed (Table 3, $p < 0.001$) but not in control subjects and this group difference was significant by Bilker's CORANOVA ($p < .005$). Thus, it appears that the emotional and cognitive features of LLD cannot be attributed simply to the presence of WMH. Rather, it appears that an interaction between discrete WMH and diffusion abnormalities in NAWM (the "tip of the iceberg phenomenon") is characteristic of the pathophysiology of LLD. Further supporting this notion was high correlation of DTI abnormalities and impaired cognitive function in the LLD group but not in controls. Specifically, highly significant associations were found between processing speed and MD in the deep WM ROI, the CC, and prefrontal WM ROI. These results add to accumulating evidence that white matter disease adversely affects cognitive status in LLD (8,43,44) and suggests that there is a contribution of microstructural abnormalities to cognitive dysfunction in addition to the contribution of WMH. The present work does not address pathophysiological mechanisms in LLD, however it suggests widespread compromise in white matter integrity. The observed correlations between WMH volume, DTI measures and cognitive status are intriguing and warrant further investigation to determine the potential for reversibility of the underlying pathophysiology.

Acknowledgments

This work was supported by a NARSAD Independent Investigator Award (YIS), MH60697 (YIS), K24 MH079510 (YIS) and NIH K23 HD053212 (JSS). Neither the granting agencies nor any other funding entity had a role in any of the following aspects of this study: design and conduct of the study; collection, management, analysis and interpretation of the data; or preparation, review, or approval of the manuscript. Authors JSS and YIS are independent of any commercial provider, had full access to all of the data in this study, and take responsibility for the integrity of the data and the accuracy of the data analysis. Dr. Sheline serves on the advisory board of E. Lilly, Inc. No author named on the title page of this study has any financial interest in the results of the study, nor any other conflict of interest relevant to the subject matter of this manuscript. We thank Anthony Durbin for help with data acquisition and data processing.

References

1. Alexopoulos GS, Murphy CF, Gunning-Dixon FM, Latoussakis V, Kanellopoulos D, Klimstra S, Lim KO, Hoptman MJ. Microstructural white matter abnormalities and remission of geriatric depression. Am J Psychiatry 2008;165:238–244. [PubMed: 18172016]
2. Nobuhara K, Okugawa G, Sugimoto T, Minami T, Tamagaki C, Takase K, Saito Y, Sawada S, Kinoshita T. Frontal white matter anisotropy and symptom severity of late-life depression: a magnetic resonance diffusion tensor imaging study. J Neurol Neurosurg Psychiatry 2006;77:120–122. [PubMed: 16361611]
3. Taylor WD, MacFall JR, Payne ME, McQuoid DR, Provenzale JM, Steffens DC, Krishnan KR. Late-life depression and microstructural abnormalities in dorsolateral prefrontal cortex white matter. Am J Psychiatry 2004;161:1293–1296. [PubMed: 15229065]
4. Sheline YI, Price JL, Vaishnavi SN, Mintun MA, Barch DM, Epstein AA, Wilkins CH, Snyder AZ, Couture L, Schechtman K, McKinstry RC. Regional white matter hyperintensity burden in automated segmentation distinguishes late-life depressed subjects from comparison subjects matched for vascular risk factors. Am J Psychiatry 2008;165:524–532. [PubMed: 18281408]
5. Basser PJ, Mattiello J, LeBihan D. Estimation of the effective self-diffusion tensor from the NMR spin echo. J Magn Reson B 1994;103:247–254. [PubMed: 8019776]
6. Beaulieu C. The basis of anisotropic water diffusion in the nervous system - a technical review. NMR Biomed 2002;15:435–455. [PubMed: 12489094]
7. Wolf PA, D'Agostino RB, Belanger AJ, Kannel WB. Probability of stroke: a risk profile from the Framingham Study. Stroke 1991;22:312–318. [PubMed: 2003301]
8. Sheline YI, Barch DM, Garcia K, Gersing K, Pieper C, Welsh-Bohmer K, Steffens DC, Doraiswamy PM. Cognitive function in late life depression: relationships to depression severity, cerebrovascular risk factors and processing speed. Biol Psychiatry 2006;60:58–65. [PubMed: 16414031]
9. Folstein MF, Robins LN, Helzer JE. The Mini-Mental State Examination. Arch Gen Psychiatry 1983;40:812. [PubMed: 6860082]
10. Montgomery SA, Asberg M. A new depression scale designed to be sensitive to change. Br J Psychiatry 1979;134:382–389. [PubMed: 444788]
11. Rowland DJ, Garbow JR, Laforest R, Snyder AZ. Registration of [18F]FDG microPET and small-animal MRI. Nucl Med Biol 2005;32:567–572. [PubMed: 16026703]
12. Tailairach, J.; Tournoux, P. Coplanar Stereotaxic Atlas of the Human Brain. New York: Thieme Medical; 1988.
13. Lancaster JL, Glass TG, Lankipalli BR, Downs H, Mayberg H, Fox PT. A modality-independent approach to spatial normalization of tomographic images of the human brain. Human Brain Mapping 1995;3:209–223.
14. Ojemann JG, Akbudak E, Snyder AZ, McKinstry RC, Raichle ME, Conturo TE. Anatomic localization and quantitative analysis of gradient refocused echo-planar fMRI susceptibility artifacts. Neuroimage 1997;6:156–167. [PubMed: 9344820]
15. Snyder, AZ. Difference image vs. ratio image error function forms in PET-PET realignment. In: Bailey, D.; Jones, T., editors. Quantification of brain function using PET. San Diego: Academic Press; 1996. p. 131-137.
16. Bezdek JC, Hall LO, Clarke LP. Review of MR image segmentation techniques using pattern recognition. Med Phys 2000;20:1033–1048. [PubMed: 8413011]
17. Styner M, Brechbuhler C, Szekely G, Gerig G. Parametric estimate of intensity inhomogeneities applied to MRI. IEEE Trans Med Imaging 2000;19:153–165. [PubMed: 10875700]
18. Van Essen DC. A Population-average Landmark- and Surface- based (PALS) atlas of human cerebral cortex. Neuroimage 2005;28:635–662. [PubMed: 16172003]
19. Bae JN, MacFall JR, Krishnan KR, Payne ME, Steffens DC, Taylor WD. Dorsolateral prefrontal cortex and anterior cingulate cortex white matter alterations in late-life depression. Biol Psychiatry 2006;60:1356–1363. [PubMed: 16876144]
20. Croxson PL, Johansen-Berg H, Behrens TE, Robson MD, Pinsk MA, Gross CG, Richter W, Richter MC, Kastner S, Rushworth MF. Quantitative investigation of connections of the prefrontal cortex in

the human and macaque using probabilistic diffusion tractography. J Neurosci 2005;25:8854–8866. [PubMed: 16192375]

21. Basser PJ. Inferring microstructural features and the physiological state of tissues from diffusion-weighted images. NMR Biomed 1995;8:333–344. [PubMed: 8739270]
22. Shimony JS, McKinstry RC, Akbudak E, Aronovitz JA, Snyder AZ, Lori NF, Cull TS, Conturo TE. Quantitative diffusion-tensor anisotropy brain MR imaging: normative human data and anatomic analysis. Radiology 1999;212:770–784. [PubMed: 10478246]
23. Bilker WB, Brensinger C, Gur RC. A Two factor ANOVA-like test for correlated correlations: CORANOVA. Multivariate Behavioral Research 2004;39:565–594.
24. Thomas AJ, O'Brien JT, Davis S, Ballard C, Barber R, Kalaria RN, Perry RH. Ischemic basis for deep white matter hyperintensities in major depression: a neuropathological study. Arch Gen Psychiatry 2002;59:785–792. [PubMed: 12215077]
25. Caramia F, Pantano P, Di Legge S, Piattella MC, Lenzi D, Paolillo A, Nucciarelli W, Lenzi GL, Bozzao L, Pozzilli C. A longitudinal study of MR diffusion changes in normal appearing white matter of patients with early multiple sclerosis. Magn Reson Imaging 2002;20:383–388. [PubMed: 12206862]
26. Ciccarelli O, Werring DJ, Barker GJ, Griffin CM, Wheeler-Kingshott CA, Miller DH, Thompson AJ. A study of the mechanisms of normal-appearing white matter damage in multiple sclerosis using diffusion tensor imaging--evidence of Wallerian degeneration. J Neurol 2003;250:287–292. [PubMed: 12638018]
27. Gallo A, Rovaris M, Riva R, Ghezzi A, Benedetti B, Martinelli V, Falini A, Comi G, Filippi M. Diffusion-tensor magnetic resonance imaging detects normal-appearing white matter damage unrelated to short-term disease activity in patients at the earliest clinical stage of multiple sclerosis. Arch Neurol 2005;62:803–808. [PubMed: 15883269]
28. Guo AC, Jewells VL, Provenzale JM. Analysis of normal-appearing white matter in multiple sclerosis: comparison of diffusion tensor MR imaging and magnetization transfer imaging. AJNR Am J Neuroradiol 2001;22:1893–1900. [PubMed: 11733323]
29. Rovaris M, Bozzali M, Iannucci G, Ghezzi A, Caputo D, Montanari E, Bertolotto A, Bergamaschi R, Capra R, Mancardi GL, Martinelli V, Comi G, Filippi M. Assessment of normal-appearing white and gray matter in patients with primary progressive multiple sclerosis: a diffusion-tensor magnetic resonance imaging study. Arch Neurol 2002;59:1406–1412. [PubMed: 12223026]
30. Corkill RG, Garnett MR, Blamire AM, Rajagopalan B, Cadoux-Hudson TA, Styles P. Multi-modal MRI in normal pressure hydrocephalus identifies pre-operative haemodynamic and diffusion coefficient changes in normal appearing white matter correlating with surgical outcome. Clin Neurol Neurosurg 2003;105:193–202. [PubMed: 12860514]
31. Haris M, Kumar S, Raj MK, Das KJ, Sapru S, Behari S, Rathore RK, Narayana PA, Gupta RK. Serial diffusion tensor imaging to characterize radiation-induced changes in normal-appearing white matter following radiotherapy in patients with adult low-grade gliomas. Radiat Med 2008;26:140–150. [PubMed: 18683569]
32. Hou DJ, Tong KA, Ashwal S, Oyoyo U, Joo E, Shutter L, Obenaus A. Diffusion-weighted magnetic resonance imaging improves outcome prediction in adult traumatic brain injury (2007). J Neurotrauma 24:1558–1569. [PubMed: 17970619]
33. Huang J, Friedland RP, Auchus AP. Diffusion tensor imaging of normal-appearing white matter in mild cognitive impairment and early Alzheimer disease: preliminary evidence of axonal degeneration in the temporal lobe. AJNR Am J Neuroradiol 2007;28:1943–1948. [PubMed: 17905894]
34. O'Sullivan M, Summers PE, Jones DK, Jarosz JM, Williams SC, Markus HS. Normal-appearing white matter in ischemic leukoaraiosis: a diffusion tensor MRI study. Neurology 2001;57:2307–2310. [PubMed: 11756617]
35. Yang Q, Huang X, Hong N, Yu X. White matter microstructural abnormalities in late-life depression. Int Psychogeriatr 2007;19:757–766. [PubMed: 17346365]
36. Yuan Y, Zhang Z, Bai F, Yu H, Shi Y, Qian Y, Zang Y, Zhu C, Liu W, You J. White matter integrity of the whole brain is disrupted in first-episode remitted geriatric depression. Neuroreport 2007;18:1845–1849. [PubMed: 18090324]

37. Alexopoulos GS, Meyers BS, Young RC, Campbell S, Silbersweig D, Charlson M. 'Vascular depression' hypothesis. Arch Gen Psychiatry 1997;54:915–922. [PubMed: 9337771]

38. Alexopoulos GS, Meyers BS, Young RC, Kakuma T, Silbersweig D, Charlson M. Clinically defined vascular depression. Am J Psychiatry 1997;154:562–565. [PubMed: 9090349]

39. Krishnan KR, Hays JC, Blazer DG. MRI-defined vascular depression (1997). Am J Psychiatry 154:497–501. [PubMed: 9090336]

40. Musselman DL, Evans DL, Nemeroff CB. The relationship of depression to cardiovascular disease: epidemiology, biology, and treatment. Arch Gen Psychiatry 1998;55:580–592. [PubMed: 9672048]

41. Taylor WD, Steffens DC, Krishnan KR. Psychiatric disease in the twenty-first century: The case for subcortical ischemic depression. Biol Psychiatry 2006;60:1299–1303. [PubMed: 17014829]

42. Steffens DC, Helms MJ, Krishnan KR, Burke GL. Cerebrovascular disease and depression symptoms in the cardiovascular health study. Stroke 1999;30:2159–2166. [PubMed: 10512922]

43. Butters MA, Whyte EM, Nebes RD, Begley AE, Dew MA, Mulsant BH, Zmuda MD, Bhalla R, Meltzer CC, Pollock BG, Reynolds CF 3rd, Becker JT. The nature and determinants of neuropsychological functioning in late-life depression. Arch Gen Psychiatry 2004;61:587–595. [PubMed: 15184238]

44. Murphy CF, Gunning-Dixon FM, Hoptman MJ, Lim KO, Ardekani B, Shields JK, Hrabe J, Kanellopoulos D, Shanmugham BR, Alexopoulos GS. White-matter integrity predicts stroop performance in patients with geriatric depression. Biol Psychiatry 2007;61:1007–1010. [PubMed: 17123478]

45. Alexopoulos GS, Kiosses DN, Choi SJ, Murphy CF, Lim KO. Frontal white matter microstructure and treatment response of late-life depression: a preliminary study. Am J Psychiatry 2002;159:1929–1932. [PubMed: 12411231]

46. Nobuhara K, Okugawa G, Minami T, Takase K, Yoshida T, Yagyu T, Tajika A, Sugimoto T, Tamagaki C, Ikeda K, Sawada S, Kinoshita T. Effects of electroconvulsive therapy on frontal white matter in late-life depression: a diffusion tensor imaging study. Neuropsychobiology 2004;50:48–53. [PubMed: 15179020]

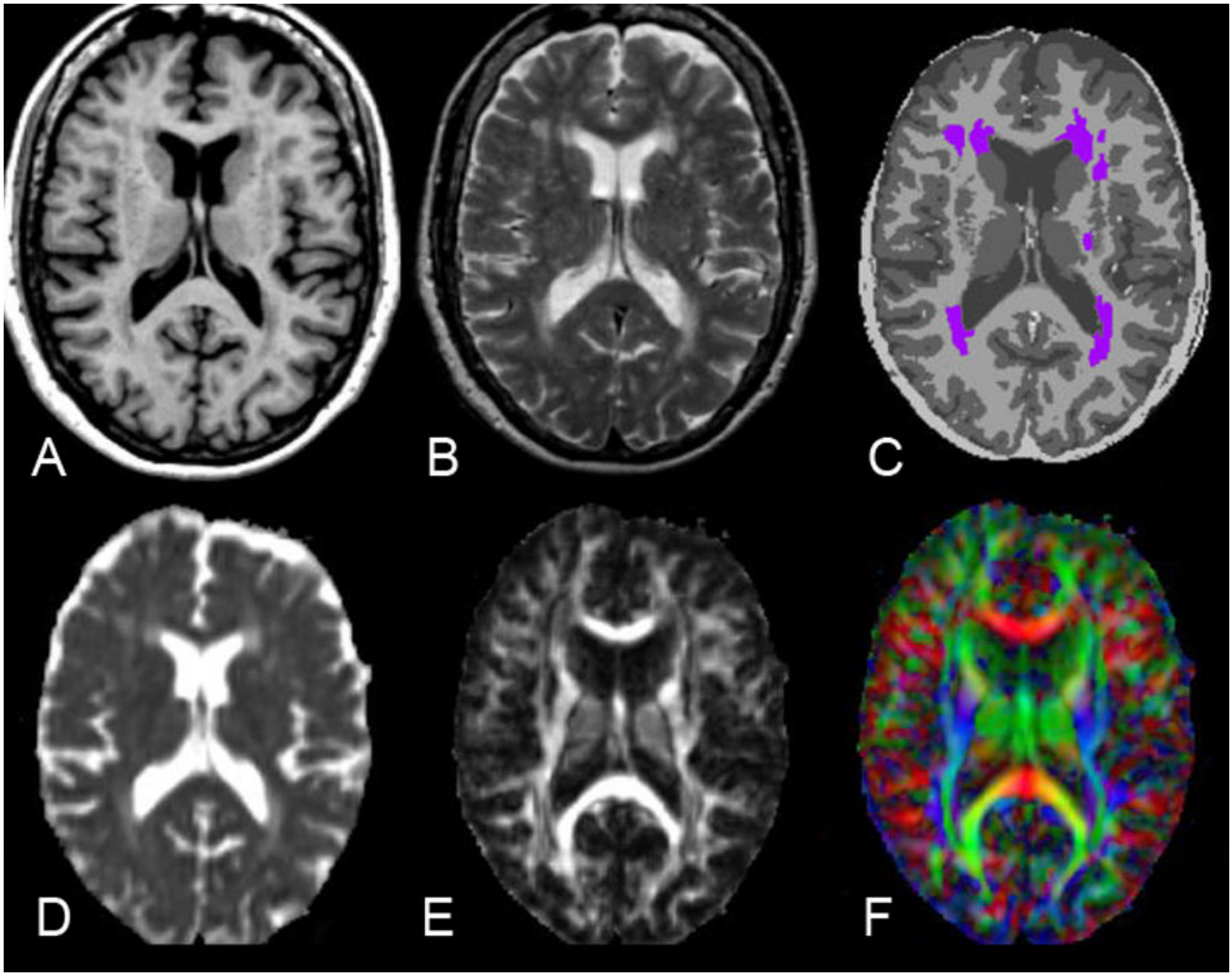

Figure 1.
Illustration of sequential image processing steps. A: T1-weighted image of one subject. B: Coregistered T2-weighted image of the same subject. C: Segmentation result. Voxels corresponding to WMH lesions are shown in purple. D: Mean diffusivity (MD). E: Relative anisotropy (RA). F: Direction of the principal axis of diffusion color-coded using the standard scheme. Red: left-right; Green: anterior-posterior; Blue: ventral-dorsal. Brightness is proportional to the square root of the relative anisotropy.

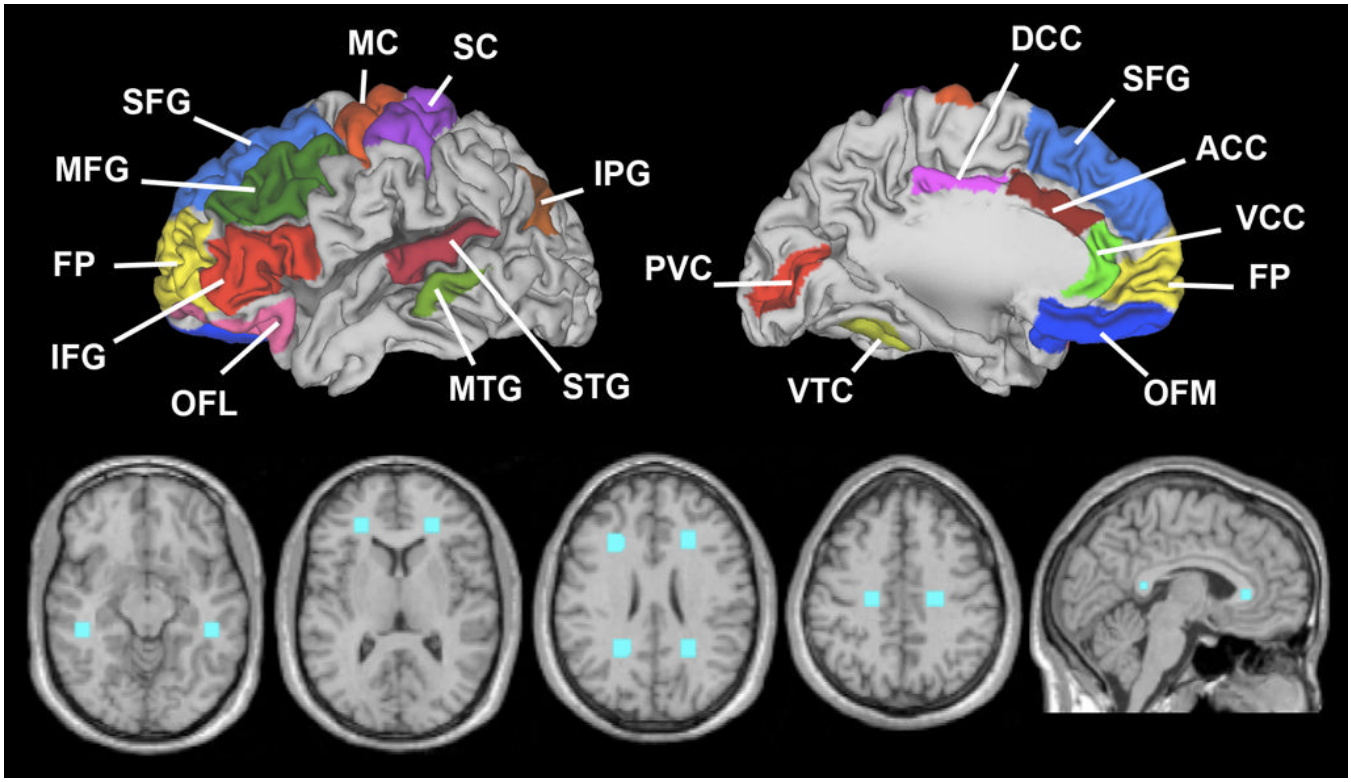

Figure 2.
Top row: Cortical (2D) ROIs defined on a population averaged landmark and surface based atlas (PALS, Van Essen 2005. SFG: superior frontal gyrus; MFG: middle frontal gyrus; IFG: inferior frontal gyrus; OFM: medial orbital frontal; OFL: lateral orbital frontal; DCC: dorsal cingulate; ACC: anterior cingulate; VCC: ventral cingulate cortex; FP: fronto-polar; MC: motor cortex; MTG: medial temporal gyrus; STG: superior temporal gyrus; VTC: ventral temporal cortex (fusiform gyrus); SC: somatosensory cortex; IPG: inferior parietal gyrus; PVC: primary visual cortex. Creation of 3D ROIs from 2D cortical patches is illustrated in Figure 3. Bottom row: Deep white matter ROIs illustrated on atlas slices. Temporal, anterior frontal, dorsal frontal, parietal posterior frontal ROIs are shown in axial views. The sagittal view shows the anterior and posterior corpus callosum ROIs.

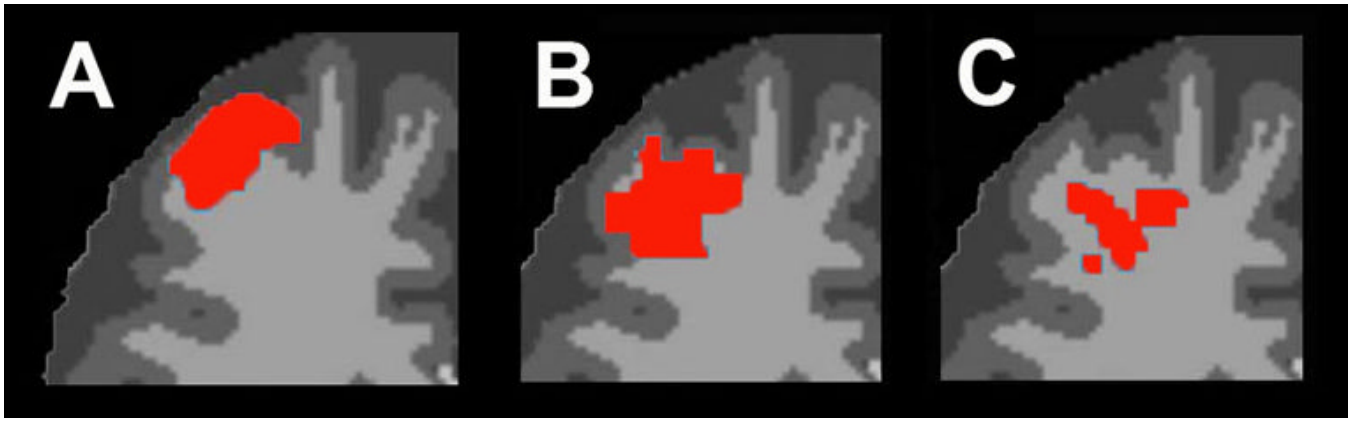

Figure 3.
Creation of individual 3D ROI in subcortical white matter from 2D atlas ROI. A: After transformation of the atlas–defined 2D region into subject data space and projection by 3mm into the white matter. B: After isotropic dilation by 2mm. C: After exclusion of gray matter by masking and additional erosion by one voxel to prevent volume averaging with gray matter.

Table 1

Demographic Information

	Depressed N=78	Control N=23	p
Gender*, n (%)			0.459
Male	24 (30.8%)	9 (39.1%)	
Female	54 (69.2%)	14 (60.9%)	
Race*, n (%)			1.000
White	71 (91.0%)	22 (95.7)	
Black	6 (7.7%)	1 (4.3%)	
Asian	1 (1.3%)	0 (0%)	
Age** Mean (SD)	68.6 (7.7)	70.0 (5.9)	0.207
Education** Mean (SD)	14.1 (2.9)	15.3 (2.6)	0.108
MADRS Score** Mean (SD)	26.9 (4.2)	(n=13) 1.8 (1.2)	< 0.001
Vascular burden**,*a* Mean (SD)	12.1 (5.1)	11.7 (3.2)	0 .555

*Fisher's exact test,

**Wilcoxon-Mann-Whitney Exact Test

*a*Vascular burden score is a composite score as described in the Framingham Study.

Table 2

Summary Statistics for Deep WM and Superficial WM (RA and MD)

	Depressed		Controls		p-value**
	N	Mean (SD)	N	Mean (SD)	
Deep WM RA	75	0.27 (0.025)	23	0.28 (0.019)	0.6931
Deep WM MD	75	0.76 (0.043)	23	0.74 (0.037)	**0.0014**
CC RA	73	0.63 (0.068)	23	0.66 (0.0557)	0.0640
CC MD	73	0.79 (0.090)	23	0.75 (0.074)	**0.0062**
Prefrontal WM RA	78	0.32 (0.027)	22	0.34 (0.027)	**0.0043**
Prefrontal WM MD	78	0.76 (0.044)	22	0.73 (0.036)	**0.0004**
Non-Prefrontal WM* RA	77	0.35 (0.031)	22	0.36 (0.026)	0.4314
Non-Prefrontal WM* MD	77	0.80 (0.037)	22	0.77 (0.033)	<**0.0001**

*Temporal+Parietal+Occipital+Motor WM

**WM Wilcoxon-Mann-Whitney exact test stratifying by age and gender

RA is dimensionless. The dimension of MD is micron squared per millisecond.

Biol Psychiatry. Author manuscript; available in PMC 2010 January 11.

Table 3

Spearman Correlation Results for WMH volume and DTI values, adjusting for age and gender

	Depressed			Controls		
	N	**Corr**	**p-values**	**N**	**Corr**	**p-values**
Deep WM RA	68	−0.28	**0.0204**	22	0.05	0.8467
Prefrontal RA	70	−0.29	**0.0158**	21	0.01	0.9741
CC RA	70	−0.19	0.1246	22	0.30	0.2036
Non-prefrontal* RA	69	−0.28	**0.0227**	21	0.13	0.5969
Deep WM MD	68	0.56	**<.0001**	22	−0.02	0.9419
Prefrontal WM MD	70	0.35	**0.0030**	21	−0.05	0.8479
CC MD	70	0.37	**0.0019**	22	−0.20	0.3928
Non-prefrontal* MD	69	0.18	0.1528	21	0.12	0.6147

*Temporal+Parietal+Occipital+Motor WM

Table 4

Table 4A. Spearman Rank-Correlation Results for Processing Speed versus DTI parameter values in different brain regions, adjusting for age and gender						
	Depressed			Controls		
	N	Corr	p-values	N	Corr	p-values
Deep WM RA	73	0.08	0.4829	23	−0.31	0.1658
Prefrontal RA	75	0.29	**0.0153**	22	−0.09	0.7097
CC RA	70	0.12	0.3130	23	0.12	0.6181
Non-prefrontal* RA	75	0.14	0.2250	22	−0.09	0.6923
Deep WM MD	73	−0.29	**0.0157**	23	0.25	0.2783
Prefrontal MD	75	−0.32	**0.0056**	22	0.29	0.2204
CC MD	70	−0.26	**0.0295**	23	0.09	0.6839
Non-prefrontal* MD	75	−0.09	0.4286	22	0.12	0.6183

Table 4B. Spearman Rank-Correlation Results for Processing Speed versus DTI parameter values in different brain regions, adjusting for age, gender, and WMH						
	Depressed			Controls		
	N	Corr	p-values	N	Corr	p-values
Deep WM RA	66	0.01	0.9100	22	−0.33	0.1659
Prefrontal RA	67	0.20	0.1079	21	−0.07	0.7889
CC RA	67	0.07	0.6005	22	0.06	0.7921
Non-prefrontal* RA	67	−0.05	0.7153	21	−0.15	0.5471
Deep WM MD	66	−0.21	0.0954	22	0.26	0.2821
Prefrontal MD	67	−0.27	**0.0337**	21	0.30	0.2280
CC MD	67	−0.19	0.1287	22	0.15	0.5407
Non-prefrontal* MD	67	−0.08	0.5458	21	0.08	0.7435

*Temporal+Parietal+Occipital+Motor WM

*Temporal+Parietal+Occipital+Motor WM

Table 5

Summary of the recent literature on DTI measurements in LLD. Articles in young depressed or with other co-morbidities were excluded. FA – Fractional anisotropy, an analogous measure of anisotropy to RA. IC – Internal Capsule, ECT – Electroconvulsive therapy, other abbreviations as in the text.

Reference	Number Subjects	DTI Value	Region Evaluated	Major Result
Alexopoulos et al., 2002 (45)	13	FA	Frontal ROI based	Low FA was associated with low remission rate
Taylor et al., 2004 (3)	33	FA	Frontal, Occipital, ROI based	Low FA in depressed, one ROI
Nobuhara et al., 2004 (46)	20	FA	Frontal, Temporal, CC, ROI based	Low FA in depressed, post ECT changes
Nobuhara et al., 2006 (2)	26	FA	Whole brain, ROI based	Low FA in depressed in the frontal and temporal
Bae et al., 2006 (19)	190	FA, MD	Frontal, IC, CC, ROI based	Low FA in depressed, no difference in MD
Yang et al., 2007 (35)	46	FA	Frontal, Temporal, CC, ROI based	Low FA in depressed in multiple regions
Murphy et al., 2007 (44)	51	FA	Whole brain, Voxel based	Low FA in depressed in multiple regions
Yuan et al., 2007 (36)	30	FA	Whole brain, Voxel based	Low FA in depressed in multiple regions
Alexopoulos et al., 2008 (1)	48	FA	Whole brain, Voxel based	Low FA decreased likelihood for remission